Electromagnon softening in a Kagome lattice at the magnetoelectric-multiferroic transition

January 7, 2009

C.P. van der Vegte
Supervisor: Maxim Mostovoy

Abstract

The magnetoelectric interactions that induce electric polarization in magnets can also couple oscillations of magnetization to polar lattice vibrations. The oscillations of polarization at magnon frequency and vice versa give rise to dynamic magnetoelectric effects, such as mixed spin-phonon excitations (electromagnons). The best systems to look for them are frustrated magnets, where competing interactions and the geometry of the spin lattice favor unconventional magnetic states. We study the spectrum electromagnons close to the magnetoelectric-multiferroic instability in the Heisenberg antiferromagnet on the Kagome lattice.

Contents

1 Introduction

Inducing magnetization with electric fields, and vice versa inducing polarization with magnetic fields is called the magnetoelectric effect. It has fascinated physicist for decades because of possible applications in multi-state memory devices and for fundamental reasons. The latter results from the complex interplay between different microscopic degrees of freedom found in magnetoelectrics and multiferroics. The magnetoelectric effect can be introduced via an expansion of the free energy [1]

$$F(\vec{E},\vec{H}) \quad = \quad F_0 - \frac{\varepsilon_{ij}E_iE_j}{8\pi} - \frac{\mu_{ij}H_iH_j}{8\pi} - \alpha_{ij}E_iH_j + ... \quad . \tag{1}$$

Here ε_{ij} is the dielectric permittivity, μ_{ij} the magnetic permittivity and α_{ij} is the magnetoelectric tensor leading to the linear magnetoelectric effect. Nonlinear terms with respect to the external fields are possible but will not be considered. Using $\partial F/\partial\vec{E} = -\vec{D}/4\pi$, $\partial F/\partial\vec{H} = -\vec{B}/4\pi$ and the standard relation between the electric field, the electric displacement field and the polarization respectively the magnetic field,the auxiliary magnetic field and the magnetization gives:

$$P_i \quad = \quad \chi^e_{ij}E_j + \alpha_{ij}H_j, \quad \chi^e_{ij} = \frac{\varepsilon_{ij}-\delta_{ij}}{4\pi}, \tag{2}$$

$$M_i \quad = \quad \alpha_{ji}E_j + \chi^m_{ij}H_j, \quad \chi^m_{ij} = \frac{\mu_{ij}-\delta_{ij}}{4\pi}, \tag{3}$$

where χ^e_{ij} and χ^m_{ij} are called respectively, the dielectric and magnetic susceptibility tensors. We use Gausian units. From these equations it can be seen that an applied electric field induces magnetization and an applied magnetic field induces polarization for nonzero α_{ij}. It follows from the Maxwell equations that under time reversal $t \to -t$ the magnetic field changes sign and the electric field remains invariant, and under spatial inversion $r \to -r$ the electric field changes sign whereas the magnetic field remains invariant. Since the free energy Eq. (1) is invariant under time reversal and spatial inversion, the magnetoelectric tensor α_{ij} should change sign under these transformations. So the magnetoelectric effect requires a simultaneous violation of time reversal and space inversion symmetry.

There is a theoretical upper bound on the magnetoelectric susceptibility.[2]The free energy given in Eq. (1) can be rewritten as

$$F(\vec{E},\vec{H}) = F_0 - \begin{pmatrix}\vec{E} & \vec{H}\end{pmatrix}\frac{1}{8\pi}\begin{pmatrix}\varepsilon & 4\pi\alpha \\ 4\pi\alpha^T & \mu\end{pmatrix}\begin{pmatrix}\vec{E}\\ \vec{H}\end{pmatrix}.$$

Thermodynamic stability requires that the free energy must have an absolute maximum when the electric and magnetic fields are zero. For this to be valid

[1] L. D. Landau and E. M. Lifshitz 1984 Electrodynamics of contiuous media

[2] W. F. Brown, R. M. Hornreich and S. Shtrikman Phys. Rev. 168 574

the 6×6 matrix in the equation above has to be positive definite which leads to an upper bound on the magnetoelectric susceptibility

$$|\alpha_{ij}| \leq \frac{\sqrt{\varepsilon_{ij}\mu_{ij}}}{4\pi}. \tag{4}$$

For materials with localized magnetic moments, the diamagnetic susceptibility is much smaller than the paramagnetic susceptibility. Since all magnetoelectric materials must be of this type of order, the diamagnetic contribution may be neglected. A stronger condition on the magnetoelectric suscepitibility can then be found.

$$\alpha_{ij} \leq \sqrt{\chi^e_{ii}\chi^m_{jj}}. \tag{5}$$

Collinear antiferromagnets in which the linear magnetoelectric effect is commonly found have a magnetic susceptibility $\chi^m \ll 1$. As a consequence the electric polarization induced by a magnetic field in these system is orders of magnitude smaller then in usual ferroelectrics.

Experimentally the magnetoelectric susceptibility α was measured for Cr_2O_3. First an external electric field was applied and the change in magnetization was measured as a function of temperature. Then an external magnetic field was applied and the change in polarization was measured for different temperatures. The results are shown in the figure below. As can be seen the magnetoelectric coefficient determined by measuring the change in polarization is the same as the magnetoelectric coefficient determined by measuring the change in magnetization which proves that the effect is linear and Eq. (1) applies to this material.

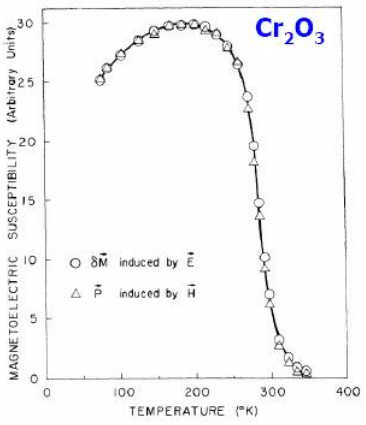

Figure 1: The magnetoelectric susceptibility of Cr_2O_3 as a function of temperature measured with two different methods. The triangles denote the change in polarization induced by an applied external magnetic field and the circles denote the change in magnetization induced by an applied external electric field.

The magnetoelectric constants of magnetoelectrics have rather low values, which makes them not very useful for applications. A stronger response is found in multiferroics, which are both electric and magnetic. In these compounds the direction of the polarization and the dielectric susceptibility can be controlled by applied magnetic fields. Below a certain temperature when spiral magnetic ordering breaks inversion symmetry, multiferroics can exhibit spontaneous magnetization and polarization simultaneously. The polarizations in these spiral magnets are however small because of the weak relativistic Dzyaloshinskii-Moriya interaction. Recently a new class of multiferroics has been identified in which non-relativistic exchange striction leads to a strong spin lattice coupling. Delaney *et al.* [3] showed that symmetry breaking in spiral magnets, and superexchange mediated spin-lattice coupling can be combined to yield materials with strong linear magnetoelectric response. They suggest that the 'KITPite' structure with chemical formula $CaAlMn_3O_7$ breaks space inversion and time reversal symmetry and predict a magnetoelectric constant 30 times larger as found in Cr_2O_3.

[3] K. T. Delaney, M. Mostovoy, N. A. Spaldin arXiv:0810.0552v1 2008

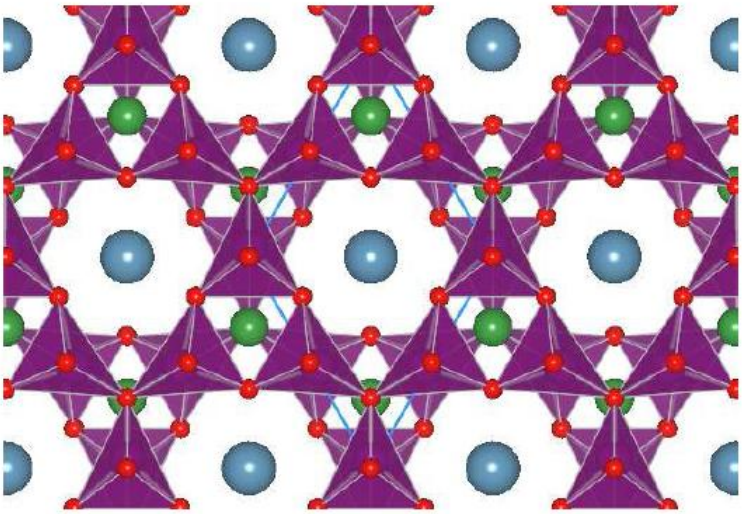

Figure 2: Two layers of KITPite in the relaxed structure. The Mn ions are at the center of the oxygen trigonal bipyramids (purple polyhedra). The correct charge balance is obtained through Ca (blue) and Al (green) counter ions situated in voids of the MnO mesh.

In this report calculations will be done for a highly frustrated spin system based on KITpite shown in figure 3. The arrows denote spins resulting from a magnetic transition metal atom with partially filled d-shells such as Mn^{3+}. The Mn atoms (blue circles) are arranged on a Kagome lattice. Oxygen ions (red circles) are positioned outside triangles pointing up and inside triangles pointing down. The manganese ions are connected by the oxygen ions that mediate superexchange.

First I consider a single spin triangle shown in figure 6. The magnetoelectric tensor α_{ij}, the dielectric permittivity ε_{ij} and magnetic permeability μ_{ij} will be calculated for the triangle by minimizing the energy in second order perturbation theory. It was found that the response functions all have a pole for a particular value of the spin lattice coupling $J_1 = J_1^{cri}$. It is expected that at this pole the material has a phase transition and becomes magnetic as well as ferroelectric.

Then elementary excitations of the Heisenberg antiferromagnet on a full Kagome lattice are discussed. The positions of the oxygen ions are assumed to be fixed and the magnonspectrum ω versus k is calculated using the semiclassical approach.

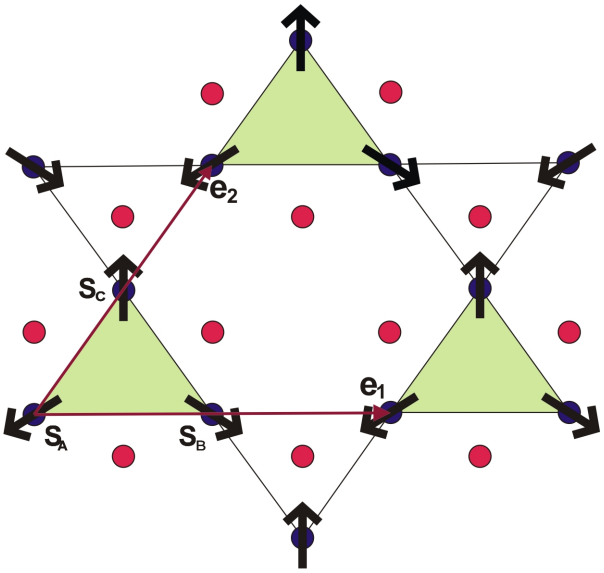

Figure 3: A highly frustrated spin system. The Mn atoms (blue circles) are arranged on a Kagome lattice with oxygen atoms (red circles) mediating the binding and superexchange

In multiferroic and magnetoelectric materials there is a strong coupling between the spin and lattice degrees of freedom which leads to electric dipole excitations of magnons, also called electromagnons. If there is a continuous phase transition into a multiferroic state, softening of a mode should be seen in the electromagnon spectrum. In section 5 I study the electromagnon spectrum with respect to the system parameters, and find that on increasing the spin lattice coupling J_1 several branches of the spectrum soften. It is remarkable to note that a particular branch softens indicating a transition for a value of $J_1 < J_1^{cri}$.

2 The model

In this section the various terms of the Hamiltonian will be explained. The Hamiltonian can be split into a part that is due to the interaction of spins and a part that is due to the lattice vibrations.

$$\mathcal{H} = \sum_{\langle ij \rangle} J(z_{ij}) \vec{S}_i \cdot \vec{S}_j + J_2 \sum_{\langle\langle ij \rangle\rangle} \vec{S}_i \cdot \vec{S}_j + \frac{D}{2} \sum_n \vec{S}_n^{z\,2} + \sum_i \frac{p_i^2}{2M} + \frac{1}{2} K \sum_i z_i^2 \quad (6)$$

Where the sum in the first term is over all nearest neighbors spins and the sum in the second term is over all next nearest neighbors. The third term is the single ion anisotropy term which represents single ion anisotropy with the xy plane as the easy plane (D>0). The fourth term contains the momentum of the oxygen ions which are allowed to move and the fith term is the harmonic oscillator term for the oxygen ions.

In the remaining part of this section I discuss the origen of the terms present in Eq. 6.

- Heisenberg Superexchange
  If orthogonal orbitals localized on atoms labelled by $i = 1, 2..$ are considered, then tunnelling between the states is described by a hopping Hamiltonian. Note that there is only one spin per site.

$$H^{(t)} = -t \sum_s (c_{i\sigma}^\dagger c_{j\sigma} + h.c.). \quad (7)$$

  If on-side Hubbard interaction is assumed

$$H_0 = U \sum_i n_{i\uparrow} n_{i\downarrow}. \quad (8)$$

  For large values of U/t, H_0 is chosen the zeroth-order Hamiltonian, with a fourfold degenerate ground state

$$\{0\} = |s_1, s_2\rangle, \quad s_i = \uparrow, \downarrow, \quad i = 1, 2. \quad (9)$$

  The energies of the doubly occupied orbitals are higher by a factor U (figure 4). From second order perturbation theory in t/U it becomes clear that the antiferromagnetic spin ordering has the lowest energy. If two neighboring spins would have been parallel the hopping can not take place because of the Pauli exclusion principle shown in figure 3. The effective Hamiltonian reduces to an isotropic antiferromagnetic Heisenberg exchange:

$$H^{(2)} = J_0 \vec{S}_1 \cdot \vec{S}_2, \quad J = \frac{4t^2}{U} \quad (10)$$

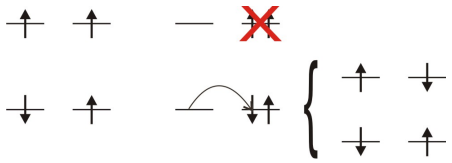

Figure 4: Spins can only hop if they are antiparallel because of the Pauli exclusion principle.

The process of virtual double occupation is called superexchange. Superexchange couplings are generated in many systems with unpaired spins. For the Kagome lattice, the unpaired spins are on the magnetic Mn^{3+} ions and there is an oxygen 'bridge' ion in between shown in figure. The superexchange constant strongly depends on the metal-oxygen-metal bond angle θ. This is because the orbital overlap between the ions changes for different θ. According to the Anderson-Kanamori-Goodenough rules [4] the exchange is antiferromagnetic for $\theta = \pi$ and ferromagnetic for $\theta = \pi/2$. In an applied magnetic field the angle between two neighbouring spins changes and so does the position of the oxygen ion. The shift of this negative oxygen ion with respect to the positively charged Mn^3+ ion induces an electric dipole moment.

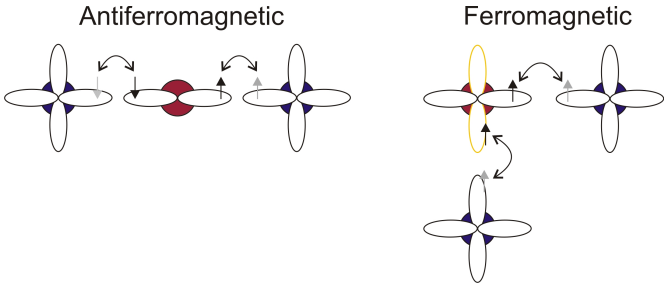

Figure 5: The exchange is antiferromagnetic if the metal-oxygen-metal angle equals π and ferromagnetic if the angle equals $\pi/2$

- Single Ion Anisotropy
  The exchange interactions explained before determine the arrangements of neighboring spins but do not fix the direction of the magnetic moments. Orbitals see the crystal through the electronic potential of the ions. The spin-orbit coupling interaction transfers the crystal environment to the spins and causes magnetic anisotropy.

[4] J. Goodenough Magnetism and the Chemical Bond 1963

3 Single spin triangle

In this section a single spin triangle with oxygen ions on the sides will be considered in order to make the physics of the model clear. I study the spin and lattice configuration in the presence of electric and magnetic fields. This analysis results in an analytic expression for the susceptibilities defined in Eq. 1. In subsection 3.1 I consider a single triangle without external fields and explicitly show that the minimal energy configuration is a 120 degrees ordering. In subsection 3.2 I use second order perturbation theory to calculate deviations of the 120 degrees ordering in the presence of external electric and magnetic fields. Throughout this section both lattice and spins are treated classically.

3.1 Single spin triangle in the absence of an external electromagnetic field

The single spin triangle is shown in the figure 6. The circles in blue are a transition metal with a partially filled d-shells for instance Mn^{3+} (S=2) and the red circles denote negative oxygen ions.

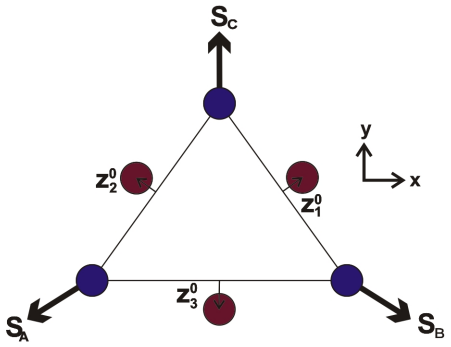

Figure 6: A single spin triangle with negative oxygen ions on the sides.

In the absence of electromagnetic fields the energy of the system equals

$$\begin{aligned}\mathcal{E}_0 &= (J_0 - J_1 z_1)(\vec{S}_B \cdot \vec{S}_C - S^2) + (J_0 - J_1 z_2)(\vec{S}_C \cdot \vec{S}_A - S^2) \\ &\quad + (J_0 - J_1 z_3)(\vec{S}_A \cdot \vec{S}_B - S^2) + \frac{1}{2} K (z_1^2 + z_2^2 + z_3^2). \end{aligned} \tag{11}$$

Because of anisotropy it that all the spins lie in the xy plane. Spins are treated classically so the inner product between spins is $\vec{S}_i \cdot \vec{S}_j = |S^2| \cos(\phi_i - \phi_j)$. The angle ϕ_i is the angle that spin S_i makes with the y-axis. The spin denoted by $\vec{S}_C$ can be chosen in the y-direction because of rotational invariance. Eq. (14) reduces to

$$\begin{aligned}\mathcal{E}_0 &= (J_0 - J_1 z_1)(S^2\cos\phi_B - S^2) + (J_0 - J_1 z_2)(S^2\cos\phi_A - S^2) \\ &\quad +(J_0 - J_1 z_3)(S^2\cos(\phi_A - \phi_B) - S^2) + \frac{1}{2}k(z_1^2 + z_2^2 + z_3^2). \qquad (12)\end{aligned}$$

The optimal configuration can be found by minimizing Eq. 15 which leads to the following five equations.

$$\frac{\partial E_0}{\partial z_1} = -J_1(S^2\cos\phi_B - S^2) + kz_1 = 0 \qquad (13)$$

$$\frac{\partial E_0}{\partial z_2} = -J_1(S^2\cos\phi_A - S^2) + kz_2 = 0 \qquad (14)$$

$$\frac{\partial E_0}{\partial z_3} = -J_1(S^2\cos(\phi_A - \phi_B) - S^2) + kz_3 = 0 \qquad (15)$$

$$\frac{\partial E_0}{\partial \phi_A} = (J_0 - J_1 z_2)(-S^2\sin\phi_A) - (J_0 - J_1 z_3)(S^2\cos(\phi_A - \phi_B)) = 0 \qquad (16)$$

$$\frac{\partial E_0}{\partial \phi_B} = (J_0 - J_1 z_1)(-S^2\sin\phi_B) + (J_0 - J_1 z_3)(S^2\cos(\phi_A - \phi_B)) = 0 \qquad (17)$$

For small values of J_1 a sollution to these equations is

$$\begin{aligned}\phi_A^0 &= \frac{4}{3}\pi, \qquad \phi_B^0 = \frac{2}{3}\pi, \quad or \qquad \phi_A^0 = \frac{2}{3}\pi, \qquad \phi_B^0 = \frac{4}{3}\pi \\ z_1^0 &= z_2^0 = z_3^0 = \frac{J_1}{k}(\frac{3}{2}S^2). \qquad (18)\end{aligned}$$

Note that due to rotational invariance all configurations with

$$|\phi_C^0 - \phi_A^0| = |\phi_C^0 - \phi_B^0| = |\phi_B^0 - \phi_A^0| = \frac{2}{3}\pi + 2\pi n \qquad (19)$$

where n is an integer, are sollutions.

3.2 Single spin triangle in a static external electric and magnetic field

In the presence of an external magnetic field the spins start to rotate which causes the oxygen ions to change position which could cause polarization. Similar an external electric field causes the the oxygen ions to shift which causes the spins to rotate which leads to magnetization. The single spin triangle in the presence of a magnetic field is shown in the figure below. The energy for the

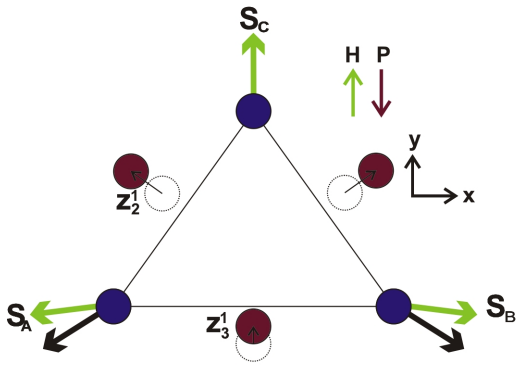

Figure 7: The single spin triangle in the presence of a magnetic field in the y-direction which causes the spins to rotate and the oxygen ions to shift.

single spin triangle is then

$$\begin{aligned}\mathcal{E} &= (J_0 - J_1 z_1)(\vec{S}_B \cdot \vec{S}_C - S^2) + (J_0 - J_1 z_2)(\vec{S}_C \cdot \vec{S}_A - S^2) \\ &\quad +(J_0 - J_1 z_3)(\vec{S}_A \cdot \vec{S}_B - S^2) + \frac{1}{2}K(z_1^2 + z_2^2 + z_3^2) \\ &\quad -\mu_0(\vec{S}_A + \vec{S}_B + \vec{S}_C) \cdot \vec{H} - q(z_1^1 - z_2^1)\frac{\sqrt{3}}{2}E_x \\ &\quad -q(\frac{z_1^1 + z_2^1}{2} - z_3)E_y. \end{aligned} \tag{20}$$

The fourth term is the interaction term of the spins with the magnetic field. The second term is the polarization in the x-direction multiplied by the electric field in the x-direction. Note that the oxygen ions are only allowed to move along the vectors $\vec{z}_i^1$

Now a magnetic field in the y-direction and an electric field in the x- and y-direction is introduced. The inner products can then be evaluated. Note that the spin $\vec{S}_C$ is parallel to the magnetic field and therefore does not change direction. If the fields are assumed to be small, second order perturbation theory can be used and the positions z_i and angles ϕ_A and ϕ_B can be expanded around the zero field sollution i.e. $\frac{4}{3}\pi, \frac{2}{3}\pi$ respectively.

$$\begin{aligned} z_i &= z_i^0 + z_i^1 \\ \phi_A &= \phi_A^0 + \triangle\phi_A \\ \cos\phi_j &\approx \cos\phi_j^0 - (\triangle\phi_j - \phi_j^0)\sin\phi_j^0 - \frac{1}{2}(\triangle\phi_j - \phi_j^0)^2\cos\phi_j^0 \end{aligned} \tag{21}$$

Filling Eq. 21 into Eq. 20 and minimizing with respect to $\triangle\phi$s and z^1's, I

obtain an expression for the susceptibilities defined in Eq. 1.

$$\begin{aligned} \varepsilon_{ii} &= \frac{3q^2\pi(-2J_0k + 3J_1^2S^2)}{4k(J_0K - 3J_1^2S^2)}, \quad \mu = \frac{-4\pi k^2\mu_0^2}{k(J_0K - 3J_1^2S^2)} \\ \alpha &= \frac{-3J_1kqS\mu_0}{2k(J_0K - 3J_1^2S^2)} \end{aligned} \tag{22}$$

Note that the dielectric permittivity, the magnetic permeability and the magnetoelectric tensor all have a pole at the same point. It is expected that a phase transition occurs in the material when this denominator equals zero.
In the energy only diagonal terms occur. This is due to the chosen ground configuration which has a so called pseudoscalar moment. If a different ground state configuration is chosen, ofdiagonal terms could occur. In the figure below this is shown for ground configuration with a toroidal moment which results in an induced polarization perpendicular to the magnetic field.

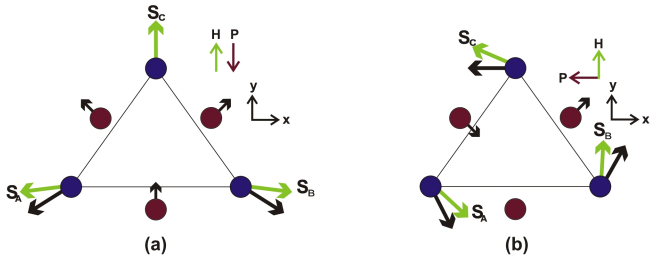

Figure 8: (a) a single spin triangle in the presence of a magnetic field in the y-direction which induces a polarization antiparallel to the field. (b) a single spin triangle with a different ground configuration in the presence of a magnetic field in the y-direction which induces a polarization perpendicular to the magnetic field.

4 Spin waves

The physics of the model is now understood by doing calculations on a single spin triangle. In this section elementary magnetic excitations of the Heisenberg antiferromagnet on a full kagome lattice shown in figure 8 will be discussed. It is important that antiferromagnetic next nearest neighbor interaction is present otherwise the spin configuration shown in the figure would not be a stable solution. Note that the positions of the oxygen ions are fixed in this section. The elementary magnetic excitations are also called spin waves or magnons. The magnon dispersion relation for ω versus k will be calculated.

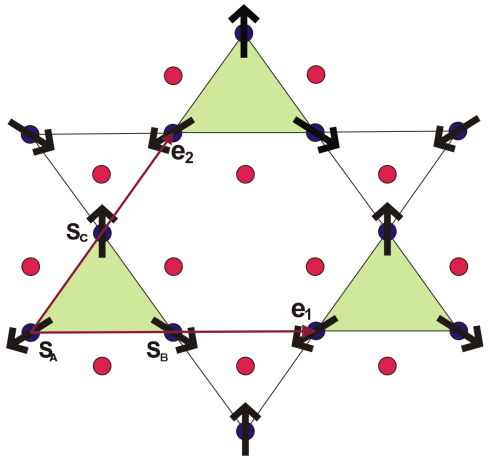

Figure 9: The Mn atoms (blue circles) are arranged on a Kagome lattice with fixed oxygen atoms (red circles). The lattice vectors are denoted by $\vec{e}_1$ and $\vec{e}_2$.

The interaction between localized spins is an exchange one

$$\mathcal{H} = J_0 \sum_{\langle nm \rangle} \vec{S}_n \cdot \vec{S}_m + J_2 \sum_{\langle\langle nm \rangle\rangle} \vec{S}_n \cdot \vec{S}_m + \frac{D}{2} \sum_n \vec{S}_n^{z\,2}, \tag{23}$$

here the sum in the fist term is the sum over all nearest neighbors, the sum in the second term is the sum over all next nearest neighbors and the third term denotes the anisotropy term. Finding the equations of motion for spins $\vec{S}_j^A$, $\vec{S}_j^B$ and $\vec{S}_j^C$ and solving these equations will give the magnon spectrum. The equations of motion will now be calculated for spin $\vec{S}_A$ using the semi-classical approach [5].

$$\frac{\hbar}{\imath} \frac{dS_j^A}{dt} = [H_i, \vec{S}_j^A] = \imath(\vec{H}_j^A \times \vec{S}_j^A), \tag{24}$$

[5] K. Yosida 1991 Theory of Magnetism

where $\vec{H}_j^A$ is the so called effective magnetic field. Using the commutation relation $[S^\alpha, S^\beta] = ie^{\alpha\beta\gamma}S^\gamma$ the commutator in Eq. 24 can be calculated.

$$[H, S_j^A] = \imath(-J_0 \sum_{\langle i \rangle} \vec{S}_i - J_2 \sum_{\langle\langle i \rangle\rangle} \vec{S}_i - DS_j^{Az}\vec{e}_z) \times \vec{S}_j^A \tag{25}$$

Spin $\vec{S}^A$ has four nearest and four next nearest neighbors. Using the lattice vectors to describe the positions of the neighbors with respect to spin $\vec{S}^A$ gives

$$\begin{aligned} \frac{\hbar}{\imath}\frac{d\vec{S}_j^A}{dt} &= \imath[-J_0(\vec{S}^B_{j+\frac{1}{2}e_1} + \vec{S}^B_{j-\frac{1}{2}e_1} + \vec{S}^C_{j+\frac{1}{2}e_1} + \vec{S}^C_{j-\frac{1}{2}e_1}) \\ &\quad -J_2(\vec{S}^B_{j-\frac{1}{2}e_1+e_2} + \vec{S}^B_{j+\frac{1}{2}e_1-e_2} + \vec{S}^C_{j-e_1+\frac{1}{2}e_2} + \vec{S}^C_{j+e_1-\frac{1}{2}e_2}) \\ &\quad -DS_j^{Az}\vec{e}_z] \times \vec{S}_j^A. \end{aligned} \tag{26}$$

The spins precess around their classical solution, now only low-energy excited states are allowed. The deviation δS_j^A may be regarded as a small quantity of the first order.

$$\vec{S}_j^A = \vec{S}^{A0} + \delta\vec{S}_j^A \tag{27}$$

Eq. 26 can then be rewritten into

$$\begin{aligned} \hbar\frac{d\delta\vec{S}_j^A}{dt} &= [2J_0(S^{B0} + S^{C0}) + 2J_2(S^{B0} + S^{C0})] \times \delta S_j^A \\ &\quad +[J_0(\delta\vec{S}^B_{j+\frac{1}{2}e_1} + \delta\vec{S}^B_{j-\frac{1}{2}e_1} + \delta\vec{S}^C_{j+\frac{1}{2}e_1} + \delta\vec{S}^C_{j-\frac{1}{2}e_1})] \times S^{A0} \\ &\quad +[J_2(\delta\vec{S}^B_{j-\frac{1}{2}e_1+e_2} + \delta\vec{S}^B_{j+\frac{1}{2}e_1-e_2} + \delta\vec{S}^C_{j-e_1+\frac{1}{2}e_2} + \delta\vec{S}^C_{j+e_1-\frac{1}{2}e_2})] \times S^{A0} \\ &\quad +[D\delta S_j^{Az}\vec{e}_z] \times S^{A0}. \end{aligned} \tag{28}$$

The Fourier-transform is defined by

$$\vec{A}_k = \frac{1}{\sqrt{N}} \sum_j e^{-\imath\vec{k}\cdot\vec{R}_j}\delta\vec{S}_j^A. \tag{29}$$

Performing the Fourier-transform on both sides of Eq. 28 gives

$$\begin{aligned} \hbar\frac{d\vec{A}_k}{dt} &= [2J_0(\vec{S}^{B0} + \vec{S}^{C0}) + 2J_2(\vec{S}^{B0} + \vec{S}^{C0})] \times \vec{A}_k \\ &\quad +[J_0(\vec{B}_k \cos\frac{k_1 a}{2} + \vec{C}_k \cos\frac{k_2 a}{2})] \times \vec{S}^{A0} \\ &\quad +[J_2(\vec{B}_k \cos(\frac{k_1 a}{2} - k_2 b) + \vec{C}_k \cos(k_1 a - \frac{k_2 a}{2}))] \times \vec{S}^{A0} \\ &\quad +[DA_k^z\vec{e}_z] \times \vec{S}^{A0}. \end{aligned} \tag{30}$$

Now the deviation A_k is split up into a perpendicular component $A_k^\perp$ and a z-component A_k^z. The cross products can then be calculated, which gives the following two equations of motion for spin S^A.

$$\begin{aligned}\hbar\frac{d\vec{A}_k^z}{dt} &= (2J_0S + 2J_2S)|A_k^\perp| \\ &\quad +(-J_0S\cos\frac{k_1a}{2} - J_2S\cos(\frac{k_1a}{2} - k_2b))|B_k^\perp| \\ &\quad +(-J_0S\cos\frac{k_2a}{2} - J_2S\cos(k_1a - \frac{k_2a}{2}))|C_k^\perp| \end{aligned} \tag{31}$$

$$\begin{aligned}\hbar\frac{d\vec{A}_k^\perp}{dt} &= (-2J_0S - 2J_2S - DS)|A_k^z| \\ &\quad +(-2J_0S\cos\frac{k_1a}{2} - 2J_2S\cos(\frac{k_1a}{2} - k_2a))|B_k^z| \\ &\quad +(-2J_0S\cos\frac{k_2a}{2} - 2J_2S\cos(k_1a - \frac{k_2b}{2}))|C_k^z| \end{aligned} \tag{32}$$

The equations of motion for spins $\vec{S}^B$ and $\vec{S}^C$ can be found using the same arguments in a similar way as done above for spin $\vec{S}^A$. Now we look for travelling wave solutions where the time dependence is of the form $e^{i\omega t}$. The equations of motion can then be written into an eigenvalue problem of the form:

$$M_{6\times6}\begin{pmatrix} A_k^z \\ A_k^\perp \\ B_k^z \\ B_k^\perp \\ C_k^z \\ C_k^\perp \end{pmatrix} = \imath\omega\hbar \begin{pmatrix} A_k^z \\ A_k^\perp \\ B_k^z \\ B_k^\perp \\ C_k^z \\ C_k^\perp \end{pmatrix}$$

This eigenvalue problem can be solved numerically. Letting the vector $\vec{k}$ 'walk' over the irreducible Brillioun zone explained in appendix A and solving for w gives the magnonspectrum. In the figure below the magnonspectrum is plotted.

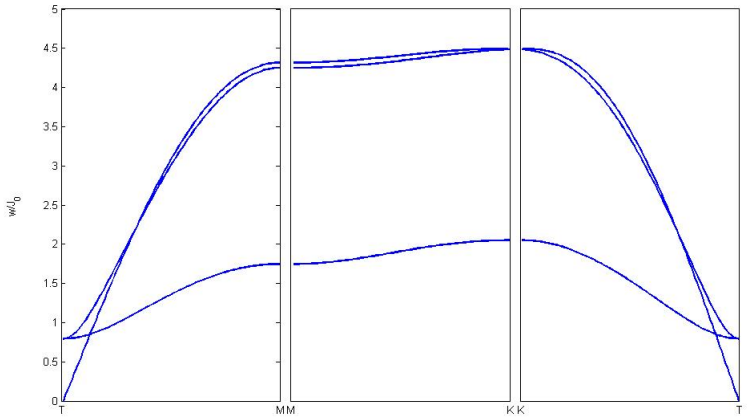

Figure 10: The magnonspectrum for $J_0 = 1$,$J_2 = 0.05$ and $D = 0.05$

If J_2 is taken larger the levels will split. For larger D the gap between the bands will increase. All branches are double degenerate.

5 Electromagnons

In multiferroic materials there is a strong coupling between the spin and lattice excitations which leads to electric dipole excitations of magnons, also called electromagnons. If there is a continuous phase transition into a multiferroic state, softening of a mode should be seen in the electromagnon spectrum. In this section the electromagnon spectrum will be calculated for the Kagome lattice shown in figure 9. The positions of the oxygen ions are now obviously not fixed. The oxygen ion denoted by number 4 is allowed to move in the x- and y-direction. The Hamiltonian is given by:

$$\begin{aligned}\mathcal{H} &= \sum_{\langle nm\rangle}(J_0 - J_1 z_{nm})\vec{S}_n \cdot \vec{S}_m + J_2 \sum_{\langle\langle nm\rangle\rangle} \vec{S}_n \cdot \vec{S}_m + \frac{D}{2}\sum_n \vec{S_n^z}^2 \\ &\quad + \sum_i \frac{p_i^2}{2M} + \sum_{\langle\rangle} \frac{1}{2} K z_{nm}^2 \end{aligned} \tag{33}$$

Where z_{nm} is the position of the oxygen ion which is in between spins $\vec{S}_n$ and $\vec{S}_m$. The summation in the first term is over all nearest neighbors, in the second term over all next nearest neighbors and in the third and the fourth term over all oxygen ions. The equations of motion for the spins can be calculated using the semi classical approach as done in the previous section.

$$\frac{\hbar}{\imath}\frac{dS_j^A}{dt} = [\mathcal{H}, \vec{S}_j] = \imath(-\sum_{\langle i\rangle}(J_0 - J_1 z_{ij})\vec{S}_i - J_2 \sum_{\langle\langle i\rangle\rangle} \vec{S}_i - D S_j^z \vec{e}_z) \times \vec{S}_j \tag{34}$$

Now it is also assumed that the oxygen ions do not differ much from there ground configuration.

$$\vec{z}_{ij} = \vec{z}_{ij}^0 + \delta\vec{z}_{ij} \tag{35}$$

Again summing over all nearest and next nearest neighbors, only keeping terms to the second order, performing the Fourier-transform and splitting up the deviation of the spins in a perpendicular and a z-component gives the equations of motion for the spins.

Since the oxygen ions are now allowed to move, their equations of motion should also be calculated. The Heisenberg equations of motion are

$$[\mathcal{H}, \vec{p}] = \frac{\hbar}{\imath}\frac{d\vec{p}}{dt} \qquad [\mathcal{H}, \vec{x}] = \frac{\hbar}{\imath}\frac{d\vec{x}}{dt}. \tag{36}$$

For the Hamiltonian considered this reduces to

$$\frac{\partial \vec{z}_{ij}}{\partial t} = \frac{\vec{p}_{ij}}{M} \tag{37}$$

$$\frac{\partial \vec{p}_{ij}}{\partial t} = -K z_{ij} - J_1 \vec{S}_i \cdot \vec{S}_j. \tag{38}$$

The equations of motion for oxygen ion 4 are split into a x- and y-component. As in the previous section, travelling wave solutions are considered where the time dependence is of the form $e^{\imath\omega t}$. The problem of solving the equations of motion can then be written in the form of an eigenvalue problem containing a 16×16 matrix. The problem is solved numerically. The electromagnonspectrum is plotted below for different values of J_1. The values used for the other variables are:

$$J_0 = 1 \qquad J_2 = 0.05 \qquad D = 0.01 \qquad S = 2 \qquad K = 10 \qquad M = 0.5 \tag{39}$$

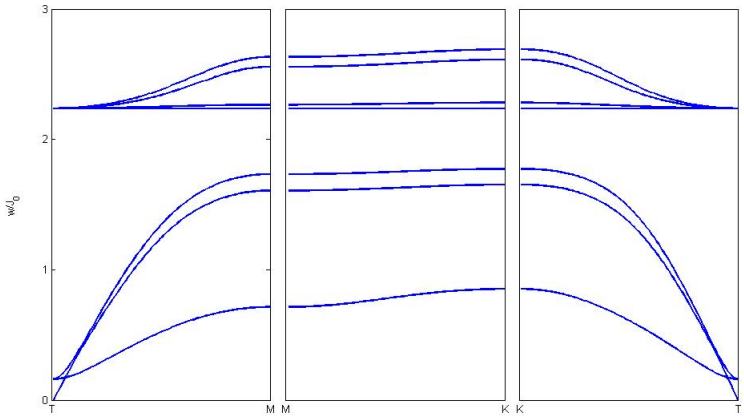

Figure 11: The electromagnonspectrum for $J_1 = 0.5$

It was expected that a phase transition would occur if the denominator of the susceptibilities in Eq. 22 equals zero. This is the case when

$$J_1^{cri} = \sqrt{\frac{J_o K}{3S^2}} \tag{40}$$

For the values taken for J_0, K, S it would mean that a phase transition would occur when $J_1 \approx 0.91$. For this value (or larger) softening of bands should be seen in the electromagnonspectrum. In figure 12 however no softening is seen. This is because the susceptibility was only calculated for a single triangle. The unit cell of the Kagome lattice however contains two triangles (one up and one down). If the full unit cell was considered, then the susceptibilities would have been proportional to:

$$\varepsilon_{ij}, \mu_{ij}, \alpha_{ij} \propto \frac{1}{-8(J_0 + J_2)K + 15J_1^2 S^2} \tag{41}$$

For the values taken this would mean that softening should be seen when $J_1^{cri} = \frac{1}{S}\sqrt{\frac{8K(J_0+J_2)}{15}} \approx 1.18$. I observe softening for a value of J_1 smaller than J_1^{cri}. The reason for this inconsistency is still an open question. One scenario is that the 120 degrees spin configuration is not the ground state for $J_1 \leq J_1^{cri}$ and a first order transition already occurs prior to $J_1 = J_1^{cri}$.

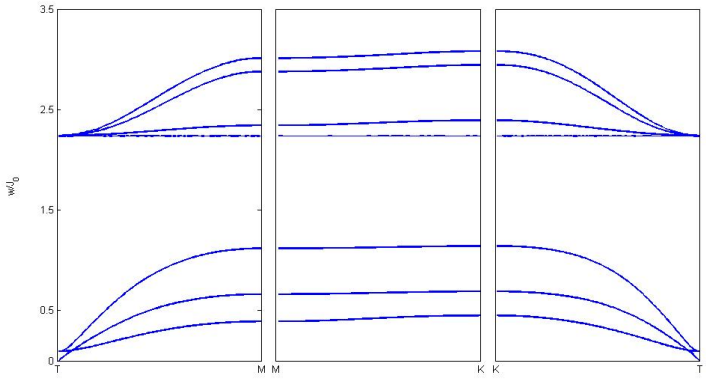

Figure 12: The electromagnonspectrum for $J_1 = 0.92$

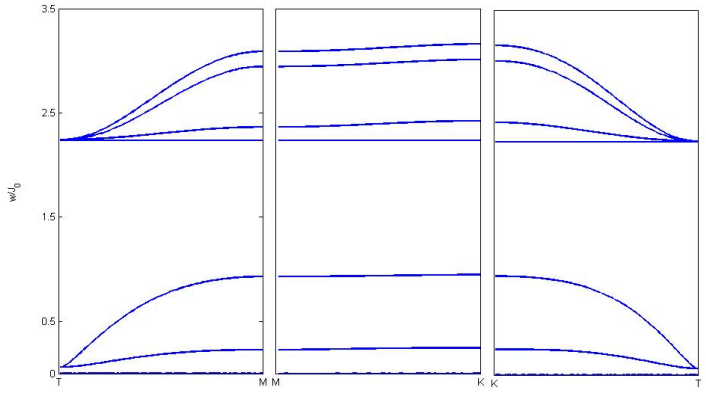

Figure 13: Softening can be seen in the electromagnonspectrum when $J_1 = 1.11$

6 Conclusions

Inversion symmetry breaking by spin ordering in frustrated magnets gives rise to a variety of interesting magnetoelectric behaviors. In materials showing the linear magnetoelectric effect an applied magnetic field induces an electric polarization proportional to the field and vice versa. The magnetoelectric interactions that induce electric polarization in magnets can also couple oscillations of magnetization to polar lattice vibrations. I have studied the spectrum of electromagnons close to the magnetoelectric-multiferroic instability in the Heisenberg antiferromagnet on the layered Kagome lattice.

First I considered a single spin triangle with Heisenberg antiferromagnet interactions between the spins and magnetostriction. I have calculated the static dielectric, magnetic and magnetoelectric susceptibilities and found that they diverge for the same values of the couplings, indicating a phase transition into a multiferroic state.

My study of the electromagnon excitation spectrum for the layered Kagome lattice shows softening of the $\vec{k} = 0$ mode for a smaller value of spin lattice coupling constant J_1 as expected from the static susceptibility calculation. The reason for this inconsistency is still an open question. One scenario is that the 120 degrees spin configuration is not the ground state for $J_1 \leq J_1^{cri}$ and a first order transition already occurs prior to $J_1 = J_1^{cri}$.

7 Appendix A: Reciprocal Space

In figure 9 the kagomé lattice is shown, the vectors e_1 and e_2 denote the unit vectors describing the lattice. Any lattice vector in real space can be written as:

$$\begin{aligned} \vec{R} &= n_1\vec{e}_1 + n_2\vec{e}_2 \\ \vec{e}_1 &= (a, 0, 0) \\ \vec{e}_2 &= (\frac{a}{2}, \frac{\sqrt{3}a}{2}, 0) \end{aligned} \tag{42}$$

Here n_i are integers. The reciprocal lattice is defined as the set all vectors $\vec{G}$ for which the following holds:

$$\begin{aligned} e^{i\vec{G}\cdot\vec{R}} &= 1 \\ \vec{G} &= m_1\vec{f}_1 + m_2\vec{f}_2 \end{aligned} \tag{43}$$

Where m_i are integers and $\vec{G}$ is any lattice vector in reciprocal space. A construction of the reciprocal lattice is given by the following equations[6].

$$\vec{f}_1 = 2\pi\frac{\vec{e}_2 \times \vec{e}_3}{\vec{e}_1 \cdot (\vec{e}_2 \times \vec{e}_3)}, \quad f_2 = 2\pi\frac{\vec{e}_3 \times \vec{e}_1}{\vec{e}_2 \cdot (\vec{e}_3 \times \vec{e}_1)} \tag{44}$$

For a two dimensional lattice, $\vec{e}_3$ is the unit vector in the z-direction. Calculating the reciprocal lattice vectors for the kagomé lattice gives

$$\vec{f}_1 = \frac{4\pi}{\sqrt{3}a}(\frac{\sqrt{3}}{2}, \frac{1}{2}, 0), \quad \vec{f}_2 = \frac{4\pi}{\sqrt{3}a}(0, 1, 0). \tag{45}$$

The reciprocal lattice is a triangular lattice. There is also periodicity in the reciprocal space. The basic cell for this periodicity is called the first Brillioun zone. Because of high symmetry, only a part of the first Brillioun zone has to be analyzed. This is the so called irreducible Brillioun zone, shown in figure 14 by the color red.

[6] C. Kittel 1997 Introduction to Solid State Physics

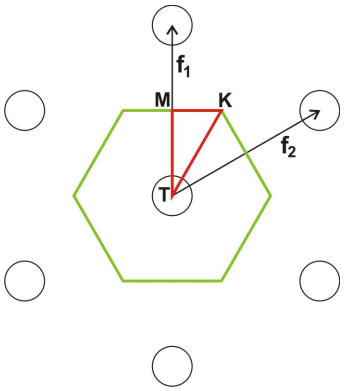

Figure 14: The reciprocal space with lattice vectors f_1 and f_2. The first Brillioun zone is drawn in green, the irreducible Brillioun zone is drawn in red.

8 Acknowledgments

In the last four months many people contributed, directly or indirectly to the success of this project. I thank them all and in particular I will mention a few. First and foremost, Maxim Mostovoy whom I have been so fortunate and proud to have as a supervisor (and taskmaster ;-)). I have always admired his teaching talents and dealing with students and science.
I am thankful to Michiel van der Vegte in a number of ways. As brothers we shared many experiences and ideas on work and less laborious matters.